MOLECULAR IMAGING OF CARDIAC METABOLISM, INNERVATION, AND CONDUCTION

Kaat Luyten, *Matthias Schoenberger

Department of Pharmaceutical and Pharmacological Sciences, University of Leuven, Leuven, Belgium
*Correspondence to Matthias.schonberger@kuleuven.be

ABSTRACT

Cardiac diseases have complex molecular origins. However, current clinical diagnostic tools are often inadequate to uncover specific molecular components of cardiac pathologies. Thus, we are still lacking a detailed understanding of disease progression, and both patient diagnosis and treatment are often inaccurate. Molecular imaging could play a leading role in translating basic research to both preclinical and clinical cardiac research, ultimately improving our understanding and management of human disease. In this review, we highlight the diversity of current molecular imaging tools that have been used in clinical research or have reached the stage of clinical translation. Facilitated by the steadily increasing infrastructure of clinical positron emission tomography and positron emission tomography-magnetic resonance imaging cameras and advancing gating analysis, these tools allow the implementation of clinical cardiac molecular imaging trials to deepen our knowledge of human disease and improve patient care.

Keywords: Positron emission tomography (PET), cardiac imaging, single photon emission computed tomography (SPECT), heart disease.

INTRODUCTION

Cardiovascular disease remains the leading cause of death in Europe and worldwide.[1] Almost all major pharmaceutical companies run large programmes on cardiovascular and cardiac drug development. Molecular imaging may play an important role in improving not only diagnosis but also treatment of cardiac diseases. The current understanding of molecular heart function is sufficient to implement more molecular imaging tools in the clinics for interrogating major aspects of cardiac function, including metabolism, innervation, and conduction. The infrastructure for clinical positron emission tomography (PET) and PET-magnetic resonance imaging is steadily growing, allowing for routine application of cardiac scans, including motion correction for heartbeat and breathing. The purpose of this review is to provide an overview of established and upcoming molecular imaging probes for cardiac function, which could aid our understanding of the human heart in health, disease, and as a function of treatment.

METABOLISM

In contrast to skeletal muscle, cardiomyocytes sustain an everlasting cycle of contraction and relaxation in order to feed our body with blood and maintain the homeostasis of nutrients and metabolic gases.[2] This highly specialised task is facilitated by a specific molecular architecture. With their steady and sustained workload, cardiomyocytes are specialised for aerobic metabolism of fatty acids (FA) and are packed with mitochondria performing oxidative phosphorylation and β-oxidation. This unique molecular architecture offers numerous opportunities to use cardiac FA metabolism as a platform for molecular imaging (Figure 1). Although cardiac metabolism has a wide adaptive capacity and plasticity when facing challenging heart energy production conditions, most forms of cardiac diseases are associated with acute or chronic changes in energy metabolism.

The heart rapidly extracts FA via either passive diffusion or a protein carrier-mediated pathway.[2,3] Oleate and palmitate are the most abundant FA in the blood pool. Once inside the cytosolic

compartment of the cardiomyocyte, FA are esterified to long-chain acyl-coenzyme A (CoA) esters by FA-CoA synthase. The activated FA can then be esterified to triacylglycerols, or transferred to carnitine via carnitine palmitoyltransferase 1 (CPT1). The acylcarnitine is then shuttled into the mitochondria by carnitine-acylcarnitine translocase, where the majority is converted back to FA-CoA by carnitine palmitoyltransferase 2 and enters mitochondrial FA β-oxidation.

Ventricular hypertrophy and dilated cardiomyopathy (DCM) are characterised by decreased myocardial capacity of FA oxidation and a shift to glucose metabolism, as a result of a decreased expression and activity of proteins involved in FA metabolism.[4,5] By contrast, diabetic cardiomyopathy results in an increase of FA oxidation due to increased circulation levels and consequential accumulation of intramyocardial lipid metabolites.[2] Ischaemic heart disease involves reduced oxidative metabolism due to reduced oxygen supply and increased anaerobic glycolysis, even though FA

oxidation recovers quickly during reperfusion following ischaemia.[2] Given this molecular pathology, current PET imaging of myocardial metabolism utilises ^{11}C-labelled natural FA and ^{18}F-labelled FA analogues, as well as the canonical [^{18}F]fludeoxyglucose.[6] For the purpose of this review, we will focus on FA metabolism, which is an independent predictor of left ventricular mass in hypertension and left ventricular dysfunction.[7]

[^{11}C]palmitate has been used to assess various steps of myocardial FA metabolism in the human heart, including storage as a triglyceride and β-oxidation (Figure 1B). Given the small storage capacities of cardiomyocytes for triglycerides and the vast number of mitochondria, the signal is dominated by the oxidation pathway and can thus be used for evaluating the enzymatic activity of CPT1, the enzyme that catalyses the acyl transfer from FA-CoA to carnitine.[8] Using this imaging probe, it has been demonstrated that obesity and diabetes mellitus (DM) are associated with an increase in myocardial FA metabolism and reduced glucose utilisation.[9,10]
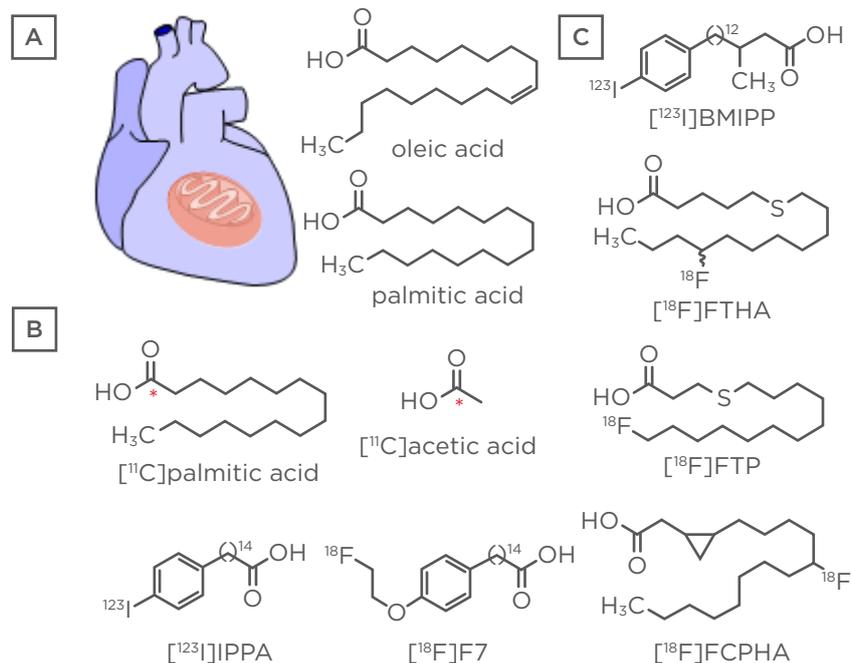
Figure 1: Cardiac fatty acid metabolism.
A) Chemical structures of native unsaturated and saturated FA, oleic acid, and palmitic acid. B) PET and SPECT radiotracers that are isotopes of native FA ([^{11}C]palmitic acid and [^{11}C]acetic acid), or mimic their metabolism ([^{123}I]IPPA and [^{18}F]F7). C) FA analogues as SPECT ([^{123}I]BMIPP) and PET ligands ([^{18}F]FTHA, [^{18}F]FTP, and [^{18}F]FCPHA) that facilitate mitochondrial trapping.
BMIPP: β-methyl-para-[^{123}I]-iodophenyl-pentadecanoic acid; F7: fluoroethoxy phenyl pentadecanoic acid; FA: fatty acid; FCPHA: fluoro-3,4-methyleneheptadecanoic acid; FTHA: fluoro-6-thia-heptadecanoic acid; FTP: fluoro-4-thia-palmitate; IPPA: pentadecanoic acid; PET: positron emission tomography; SPECT: single photon emission computed tomography.

By contrast, patients with idiopathic DCM exhibited alterations in myocardial metabolism characterised by decreased FA oxidation and increased glucose metabolism.[11] Thus far, the routine clinical use of [11C]palmitate has been limited by its relatively complicated synthesis and a need for an on-site cyclotron. Recent efforts to improve synthesis and a growing infrastructure of hospital cyclotrons may facilitate future clinical use of this radiotracer.[12]

Analogously to FA, acetate is rapidly extracted by cardiomyocytes and oxidised in mitochondria via the tricarboxylic acid (TCA) cycle to CO_2 and H_2O.[13] [11C]acetate has been used to measure myocardial blood flow in patients with hypertrophic cardiomyopathy[14] and enabled simultaneous quantification of myocardial perfusion, oxidative metabolism, cardiac efficiency, and pump function at rest as well as during exercise in athletes.[15]

15-(p-[123I]iodophenyl)-pentadecanoic acid ([123I]IPPA) was the first single photon emission computed tomography (SPECT) ligand to image myocardial FA metabolism *in vivo*, showing rapid accumulation in the heart and similar clearance kinetics as palmitate, which are directly correlated with β-oxidation in animal disease models and in humans.[16,17] Currently, [123I]IPPA is commercially available in Europe and Canada, and its usefulness as a cardiac imaging agent has been explored in clinical trials.

Tu et al.[18] designed an [18F]-labelled radiotracer, 15-(4-(2-[18F]fluoroethoxy)phenyl)pentadecanoic acid ([18F]F7), based on [123I]IPPA. [18F]F7 is capable of mimicking [11C]palmitate with regard to its ability to capture all key aspects of FA metabolism, including uptake, β-oxidation, and storage as a triglyceride. In addition, it is more feasible for clinical use due to the longer half-life of [18F], and it allows quantitative PET imaging with improved temporal resolution compared to SPECT. Small animal PET studies in Sprague-Dawley rats displayed high uptake in the heart, good imaging contrast over blood and other tissues, and similar biphasic washout kinetics as [11C]palmitate.

In addition to isotopes of native FA, FA analogues acting as false substrates or inhibitors of FA metabolism have been explored as PET and SPECT ligands, whose signal emphasises myocardial β-oxidation (Figure 1C). These analogues are recognised by the cytoplasmic acyl-CoA synthase and CPT1 in the mitochondrial membrane but are trapped inside the mitochondria due to incomplete β-oxidation.

For example, β-methyl-p-[123I]-iodophenyl-pentadecanoic acid ([123I]BMIPP) has been developed as a derivative of the aforementioned [123I]IPPA with the intention of preventing β-oxidation by blocking the β-position with a methyl functional group, thus enforcing accumulation in mitochondria. [123I]BMIPP imaging has been used for identifying patients with recent exercise-induced myocardial ischaemia[19] and non-invasive diagnosis of coronary artery disease in patients with heart failure.[20]

Pandey et al.[21] investigated long-chain [18F] fluorothia FA for their use as myocardial β-oxidation probes. CoA thioesters of 4-thia FA analogues are potent inhibitors of β-oxidation through inhibition of acyl-CoA dehydrogenase, thus leading to an accumulation of radiotracers in the mitochondria after incomplete β-oxidation.[22-24]

14(R,S)-[18F]Fluoro-6-thia-heptadecanoic acid ([18F]FTHA) uptake was reduced by 81% in mice after pharmacological inhibition of CPT1 using 2-[5-(4-chlorophenyl)pentyl]-2-oxiranecarboxylate.[25] Likewise, β-oxidation inhibition by lactate infusion in pigs reduced the myocardial [18F]FTHA signal by 89%, demonstrating that nearly all of the PET ligand taken up by the heart enters the mitochondria.[26,27] Both studies confirmed that the unidirectional uptake rate of [18F]FTHA reflects β-oxidation and allows the measurement of cardiac FA-metabolism *in vivo*, which has been exploited in numerous clinical studies. For example, accumulation of [18F]FTHA in the myocardium was increased by aerobic exercise in human volunteers due to increased energy demand.[28] In patients with coronary artery disease, [18F]FTHA imaging displayed a reduced signal in accordance with reduced oxidative metabolism.[29] In addition, the [18F]FTHA signal was reduced in healthy volunteers with glucose/insulin clamp, demonstrating the ability to detect a change in energy substrate preference from FA to glucose.[30] Furthermore, [18F]FTHA has recently been used to investigate the role of metabolic alterations in the development of a maladaptive right ventricular response in pulmonary arterial hypertension.[31]

Following the same chemical strategy of inhibiting β-oxidation, 16-[18F]fluoro-4-thia-palmitate ([18F] FTP) was developed to improve sensitivity to changes in FA oxidation caused by hypoxia,

and was found to have prolonged myocardial retention.[32] [18F]FTP showed reduced FA oxidation in hypoxic rat hearts, showing comparable imaging qualities as [18F]FTHA in swine, but was not influenced by altered plasma substrate levels.[33] Elevated uptake of [18F]FTP was found in patients with Type 2 DM.[34] This is in line with the aforementioned increase in myocardial FA oxidation found in this patient group using [11C]palmitate.

Shoup et al.[35] introduced trans-9-[18F]fluoro-3,4-methyleneheptadecanoic acid ([18F]FCPHA), which features a cyclopropyl group to block β-oxidation, as a new radiolabelled FA analogue. [18F]FCPHA revealed fast blood clearance, high myocardial uptake, and good retention in rats and rhesus monkeys. [18F]FCPHA is currently undergoing a Phase II clinical trial to assess myocardial FA perfusion and uptake in coronary artery disease patients.[36]

INNERVATION

Heart function is controlled by the autonomous nervous system (Figure 2). While cholinergic neurons dominate innervation to the sinoatrial node, setting a constant rhythm of contractions,[37] adrenergic fibres predominantly innervate the ventricles.[38] Adrenergic activity induces several cardiovascular effects, including an increase in cardiac contractility (inotropy), frequency (chronotropy), rate of relaxation (lusitropy), and acceleration of impulse conduction through the atrioventricular node (dromotropy).[39] These effects are triggered by the catecholamine neurotransmitters noradrenaline and adrenaline acting on β_1-adrenergic receptors.[38]

The importance of the sympathetic nervous system in cardiac disorders, including ischaemic heart disease and heart failure, is well established.[40] Aberrant adrenergic function, including increased neurotransmitter release and reduced reuptake, occurs early in the development of heart failure as a compensatory mechanism for sustaining the cardiac output despite, for instance, a physical insult to the myocardium or increased peripheral resistance. However, if increased activity persists over time, the heart will progress into a state of chronic decompensated heart failure, and the hyperactive adrenergic activity will continue to stimulate the heart to work at a level much higher than the cardiac muscle can handle.[38]
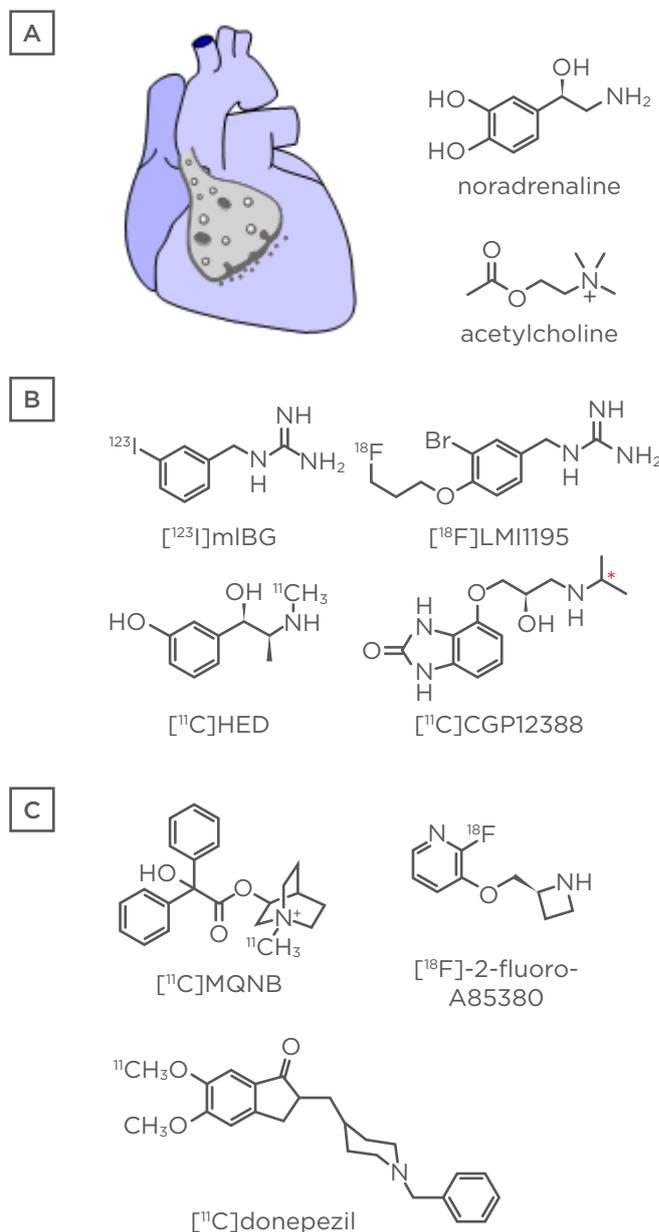
Figure 2: Cardiac innervation.
A) The heart is innervated by sympathetic and parasympathetic neurons, which signal through the neurotransmitters noradrenaline and acetylcholine, respectively. B) SPECT and PET radiotracers for assessing adrenergic innervation by measuring the presynaptic NAT ([123I]mIBG, [11C]HED, and [18F]LMI1195) and β_1-receptors ([11C]CGP12388). C) PET radiotracers for assessing parasympathetic innervation of the heart by measuring muscarinic receptors ([11C]MQNB), nicotinic $\alpha_4\beta_2$ receptors ([18F]-2-fluoro-A85380), and AChE ([11C]donepezil). AChE: acetylcholinesterase; mIBG: meta-[123I]iodobenzylguanidine; MQNB: N-[11C]methyl-quinuclidin-3-yl benzilate; NAT: noradrenaline transporter; PET: positron emission tomography; SPECT: single photon emission computed tomography.

This pathological adrenergic innervation can be measured using molecular imaging, for example SPECT and PET. Even though the cardiac specific isoforms of proteins involved in adrenergic signalling would allow, in theory, the development of dedicated and cardiac-specific imaging tools, the current toolbox is centred on general mimetics of the native neurotransmitters (Figure 2B).

Meta-[123I]iodobenzylguanidine ([123I]mIBG), an iodinated adrenergic neurotransmitter analogue, is commonly used for SPECT imaging of the presynaptic noradrenaline transporter (NAT).[41] NAT is a transmembrane protein that functions as a rapid noradrenaline reuptake system located at or near presynaptic terminals, and terminates noradrenergic signaling.[42] The cardiac signal of [123I]mIBG is lower in individuals with heart failure due to a higher NAT occupancy, allowing the use of [123I]mIBG as an independent predictor of heart failure progression and cardiac mortality. [123I]mIBG has been used clinically in different continents for almost three decades.[43-45]

In order to make adrenergic innervation imaging available for quantitative and non-invasive PET imaging, ^{11}C and ^{18}F-labelled ligands have been developed (Figure 2B). For example, [11C]meta-hydroxyephedrine ([11C]HED) was developed based on metaraminol,[46] a synthetic false transmitter analogue of noradrenaline, which is transported by NAT. It is, however, resistant to catechol-O-methyl transferase and monoamine oxidase metabolism and is thus retained in nerve terminals due to continuous cyclical release and reuptake.[47] [11C]HED displayed a lower myocardial signal in patients with congestive heart failure,[48] which correlated to patient prognosis.[49] The ^{18}F-labelled N-[3-bromo-4-(3-[18F]-fluoro-propoxy)-benzyl-guanidine ([18F]LMI1195) is structurally related to [123I]mIBG and showed a reduced signal in rodent models of heart failure.[50] Additionally, first-in-human clinical trials showed its potential for assessing myocardial sympathetic activity *in vivo*.[51] The sensitive and quantitative PET imaging using [11C]HED and [18F]LMI1195 allowed evaluation of regional denervation and heterogeneity of innervation in the heart, and could be used for predicting sudden cardiac death.[48,51]

Following the chemical design of [123I]mIBG, ^{18}F-labelled benzylguanidines (meta-[18F]fluorobenzylguanidine ([18F]mFBG)[52] and para-[18F]fluorobenzylguanidine ([18F]pFBG)) have been developed as alternative probes for imaging NAT using PET.[53,54] Both candidates have been successfully tested in neuroendocrine tumour mouse models but not yet for sympathetic nervous system dysfunction in cardiovascular diseases.

As a consequence of sustained enhanced sympathetic stimulation, postsynaptic β-adrenoceptors are downregulated in heart failure.[55,56] The recently disclosed ^{11}C-labelled beta-blocker S-4-(3-([11C]-isopropylamino)-2-hydroxypropoxy)-2H-benzimidazol-2-one ([11C]CGP12388) (Figure 2B) allowed measurements of postsynaptic β_1-receptor density and occupancy in patients with idiopathic DCM.[57] Thus, the current molecular imaging toolbox for sympathetic innervation enables measurements of all major pre and postsynaptic components of cardiac adrenergic signalling in humans. Given the widespread use of beta-blockers, it will be interesting to interrogate receptor dynamics as a function of (long-term) treatment.

Abnormal function of the parasympathetic system, in particular parasympathetic withdrawal, has been recognised as a key component of the molecular pathology underlying heart disease.[58,59] The highly specific muscarinic acetylcholinergic antagonist N-[11C]methyl-quinuclidin-3-yl benzilate ([11C]MQNB) has been used to measure myocardial muscarinic acetylcholine receptor (mAChR) density *in vivo* (Figure 2C).[60] [11C]MQNB measurements in idiopathic DCM patients revealed an upregulation of myocardial mAChR, presumably as an adaptive mechanism to β-adrenergic stimulation.[61] Likewise, patients with myocardial infarction showed increased [11C]MQNB signal in non-damaged left ventricular regions.[62] Since there is a decreased vagal tone in these pathologies, the role of upregulated expression of mAChR has still to be elucidated, and molecular imaging could play an integral role in understanding the dynamics between sympathetic and parasympathetic signalling in humans.

Acetylcholinesterase (AChE) inhibitors, such as pyridostigmine, have been used as parasympathomimetica, for instance in chronic heart failure patients.[63] Gjerløff et al.[64] tested [11C]donepezil for measurements of AChE density in human peripheral organs and found a homogenous and displaceable signal of the tracer in the left ventricle of the heart, which might help in understanding the role of neurotransmitter metabolism in human disease (Figure 2C).
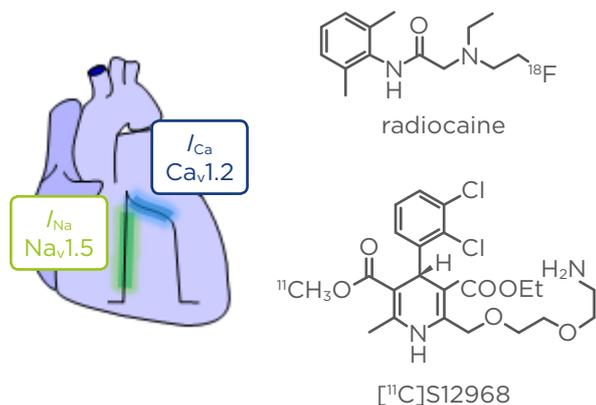
Figure 3: Cardiac conduction.
Electrical signalling through the myocardium couples excitation to contraction by the action of voltage-gated ion channels. Radiocaine imaging allows quantifying cardiac voltage-gated sodium channels *in vivo* using PET. The dihydropyridine derivative [^{11}C]S12968 enables measurements of L-type calcium channels in the heart.
PET: positron emission tomography.

Imaging of nicotinic AChR could help in better understanding their pathophysiological role in atherosclerotic disease progression and could thus be used as a diagnostic tool to risk-stratify patients for myocardial infarction and stroke.[65,66] [^{18}F]-2-fluoro-A85380 was the first PET radiotracer developed for imaging of the cardiac $\alpha_4\beta_2$-nicotinic AChR in healthy subjects and has already been tested in patients with Parkinson's disease and patients with multiple system atrophy (Figure 2C).[67]

Given the currently available imaging technology for muscarinic and nicotinic receptors, as well as AChE, understanding the dynamics of different components of the cholinergic innervation system in humans is within reach and would provide major scientific and clinical impact at relatively low risk of failure.

MYOCARDIAL CONDUCTION

The neuronal input from sympathetic and parasympathetic transmission is translated into cardiac action through a series of ion channels that respond to changes in membrane potential and ultimately couple excitation to contraction (EC-coupling).[68]

Fast activating voltage-gated sodium channels (Na$_V$s), mainly Na$_V$1.5 (SCN5A), initiate action potentials and strongly depolarise cardiomyocytes (Figure 3).[69] Subsequent activation of high-voltage activated Ca^{2+} channels (L-type, mainly Ca$_V$1.2) leads to Ca^{2+} influx and further Ca^{2+} release from the sarcoplasmic reticulum, which increases the cytosolic Ca^{2+} concentration from nanomolar to micromolar concentrations.[70] This increase elicits conformational changes of the filament complex to facilitate the actin-myosin interaction and attains myocardial contraction.[68]

Numerous cardiac diseases are rooted in abnormal electrical signalling of the myocardium due to mutated ion channels or pathological expression levels.[71] Heterozygous mutations in *SCN5A* have been implicated in rare genetic arrhythmia, such as Brugada syndrome, long-QT syndrome, and progressive cardiac conduction defect. Abnormal expression levels of SCN5A have also been found in structural heart disease, including heart failure and ischaemic cardiomyopathy.[72] Furthermore, an increase in dihydropyridine (DHP) receptor expression, an L-type calcium channel, has been found in hypertrophied hearts.[73]

Recently, the first PET radiotracer for *in vivo* molecular imaging of cardiac SCN5A has been developed (Figure 3).[74] Radiocaine, an analogue of the classical Class-1b antiarrhythmic lidocaine, allows *in vivo* measurements of density and drug occupancy of cardiac SCN5A, which, to date, could only be determined invasively or through *in vitro* methods. Specific binding to SCN5A has been demonstrated in living rats and baboons; furthermore, autoradiography studies using myocardial tissue from human failing heart explants revealed reduced target density.

In order to assess changes in L-type calcium channel density *in vivo*, several DHP-based drugs have been radiolabelled with ^{11}C for PET imaging (Figure 3).[75] The amlodipine analogue [^{11}C]S12968 showed ≤80% specific binding in the myocardium and was used for *in vivo* measurement of myocardial DHP binding site density in beagles, with low doses of Ca^{2+} channel antagonists.

The ability to measure both Na$_V$s and Ca$_V$s as determining components of the EC-coupling opens the door for future clinical studies, which will precisely identify the molecular dynamics of myocardial ion channel signalling in human disease.

Table 1: Summary of molecular imaging tools and their (bio)medical application(s).

Radioligand	Imaging of	Application
Metabolism		
[18F]FDG	Glucose uptake and retention	Myocardial viability[6]
[11C]palmitate	FA uptake, β-oxidation, and storage	Diabetes mellitus,[9,10] idiopathic DCM[11]
[11C]acetate	TCA cycle flux	Hypertrophic cardiomyopathy[14]
[123I]IPPA	FA uptake, β-oxidation, and storage	Coronary artery disease, ischaemia[17]
[18F]F7*	FA uptake, β-oxidation, and storage	*Coronary artery disease,[18] ischaemia*
[123I]BMIPP	FA storage	Exercise-induced ischaemia,[19] coronary artery disease[20]
[18F]FTHA	FA uptake and β-oxidation	Coronary artery disease,[29] pulmonary arterial hypertension[31]
[18F]FTP	FA uptake and β-oxidation	Type 2 diabetes mellitus[34]
[18F]FCPHA	FA uptake and β-oxidation	Coronary artery disease[36]
Innervation		
[123I]mIBG	Presynaptic NAT, sympathetic innervation	Congestive heart failure[43-45]
[11C]HED	Presynaptic NAT, sympathetic innervation	Congestive heart failure[48,49]
[18F]LMI1195**	Presynaptic NAT, sympathetic innervation	*Congestive heart failure[51]*
[18F]mFBG, [18F]pFBG*	Presynaptic NAT, sympathetic innervation	*Congestive heart failure[53,54]*
[11C]CGP12388	β$_1$-receptors, sympathetic innervation	Idiopathic DCM[57]
[11C]MQNB	Muscarinic receptors, parasympathetic innervation	Idiopathic DCM,[61] myocardial infarction[62]
[11C]donepezil**	AChE, acetylcholine metabolism	*Congestive heart failure[64]*
[18F]-2-fluoro-A85380**	Nicotinic α$_2$β$_4$ receptors, parasympathetic innervation	*Atherosclerosis[67]*
Myocardial conduction		
Radiocaine*	Na$_v$1.5 (SCN5A)	*Brugada syndrome,[74] LQT syndrome, progressive cardiac conduction defect*
[11C]S12968*	LTCC	*Hypertrophic cardiomyopathy[75]*

*Only tested in animal models; **only tested in first-in-human clinical trials; potential future applications in italics.

AChE: acetylcholinesterase; DCM: dilated cardiomyopathy; FA: fatty acid; LTCC: L-type calcium channel; Na$_v$: voltage-gated sodium channels; NAT: noradrenaline transporter; TCA: tricarboxylic acid; LQT: long-QT.

PERSPECTIVE

Taken together, there is a wealth of well-understood tools for *in vivo* molecular imaging of cardiac function and health, including oxidative metabolism, adrenergic and cholinergic innervation, and myocardial electrical conduction (Table 1). The majority of these tools have already been validated in humans, displaying minor radiation exposure, or have reached the stage of clinical translation, allowing widespread clinical studies in the future. Further evaluation in clinical trials will provide data on the impact of molecular imaging on changing diagnosis, treatment, and prognosis. We are convinced that the growing infrastructure of clinical PET magnetic resonance cameras will play an integral role in expanding the use of molecular imaging in cardiology, in particular with recent advances in cardiac gating reconstruction.[76] The combined information of structural integrity and changes in the cardiac molecular machinery will not only yield impactful insights in basic research but will also improve individualised patient care.

REFERENCES

1. World Health Organization. World Health Statistics 2017. Available at: http://www.who.int/gho/publications/world_health_statistics/2017. Last accessed: 25 August 2017.

2. Lopaschuk GD et al. Myocardial fatty acid metabolism in health and disease. Physiol Rev. 2010;90(1):207-58.

3. Kolwicz SC Jr et al. Cardiac metabolism and its interactions with contraction, growth, and survival of cardiomyocytes. Circ Res. 2013;113(5):603-16.

4. Neglia D et al. Impaired myocardial metabolic reserve and substrate selection flexibility during stress in patients with idiopathic dilated cardiomyopathy. Am J Physiol Heart Circ Physiol. 2007;293(6):H3270-8.

5. Sack MN et al. Fatty acid oxidation enzyme gene expression is downregulated in the failing heart. Circulation. 1996;94(11):2837-42.

6. Kobylecka M et al. Myocardial viability assessment in 18FDG PET/CT study (18FDG PET myocardial viability assessment). Nucl Med Rev Cent East Eur. 2012;15(1):52-60.

7. de las Fuentes L et al. Myocardial fatty acid metabolism: Independent predictor of left ventricular mass in hypertensive heart disease. Hypertension. 2003;41(1):83-7.

8. Bonnefont JP et al. Carnitine palmitoyltransferases 1 and 2: Biochemical, molecular and medical aspects. Mol Aspects Med. 2004;25 (5-6):495-520.

9. Peterson LR et al. Effect of obesity and insulin resistance on myocardial substrate metabolism and efficiency in young women. Circulation. 2004;109(18):2191-6.

10. Herrero P et al. Increased myocardial fatty acid metabolism in patients with type 1 diabetes mellitus. J Am Coll Cardiol. 2006;47(3):598-604.

11. Dávila-Román VG et al. Altered myocardial fatty acid and glucose metabolism in idiopathic dilated cardiomyopathy. J Am Coll Cardiol. 2002; 40(2):271-7.

12. Amor-Coarasa A et al. Synthesis of [11C]palmitic acid for PET imaging using a single molecular sieve 13X cartridge for reagent trapping, radiolabeling and selective purification. Nucl Med Biol. 2015;42(8):685-90.

13. Randle PJ et al. Control of the tricarboxylate cycle and its interactions with glycolysis during acetate utilization in rat heart. Biochem J. 1970;117(4): 677-95.

14. Timmer SAJ et al. Potential of [11C] acetate for measuring myocardial blood flow: Studies in normal subjects and patients with hypertrophic cardiomyopathy. J Nucl Cardiol. 2010; 17(2):264-75.

15. Sorensen J et al. Simultaneous quantification of myocardial perfusion, oxidative metabolism, cardiac efficiency and pump function at rest and during supine bicycle exercise using 1-11C-acetate PET-a pilot study. Clin Physiol Funct Imaging. 2010;30(4):279-84.

16. Reske SN. 123I-phenylpentadecanoic acid as a tracer of cardiac free fatty acid metabolism. Experimental and clinical results. Eur Heart J. 1985;6 (Suppl B): 39-47.

17. Richter WS et al. Combined thallium-201 and dynamic iodine-123 iodophenylpentadecanoic acid single-photon emission computed tomography in patients after acute myocardial infarction with effective reperfusion. Clin Cardiol. 2000;23(12):902-8.

18. Tu Z et al. Synthesis and evaluation of 15-(4-(2-[18F]Fluoroethoxy)phenyl) pentadecanoic acid: A potential PET tracer for studying myocardial fatty acid metabolism. Bioconjug Chem. 2010;21(12):2313-9.

19. Dilsizian V et al. Metabolic imaging with beta-methyl-p-[(123)i]-iodophenyl-pentadecanoic acid identifies ischemic memory after demand ischemia. Circulation. 2005;112(14):2169-74.

20. Abe H et al. Non-invasive diagnosis of coronary artery disease by 123I-BMIPP/201TlCl dual myocardial SPECT in patients with heart failure. Int J Cardiol. 2014;176(3):969-74.

21. Pandey MK et al. Structure dependence of long-chain [18F] fluorothia fatty acids as myocardial fatty acid oxidation probes. J Med Chem. 2012;55(23):10674-84.

22. Hovik R et al. Effects of thia-substituted fatty acids on mitochondrial and peroxisomal beta-oxidation. Studies in vivo and in vitro. Biochem J. 1990; 270(1):167-73.

23. Lau SM et al. The reductive half-reaction in Acyl-CoA dehydrogenase from pig kidney: studies with thiaoctanoyl-CoA and oxaoctanoyl-CoA analogues. Biochemistry. 1988;27(14): 5089-95.

24. Lau SM et al. 4-Thia-trans-2-alkenoyl-CoA derivatives: properties and enzymatic reactions. Biochemistry. 1989;28(20):8255-62.

25. DeGrado TR et al. 14(R,S)-[18F]fluoro-6-thia-heptadecanoic acid (FTHA): Evaluation in mouse of a new probe of myocardial utilization of long chain fatty acids. J Nucl Med. 1991;32(10):1888-96.

26. Stone CK et al. Myocardial uptake of the fatty acid analog 14-fluorine-18-fluoro-6-thia-heptadecanoic acid in comparison to beta-oxidation rates by tritiated palmitate. J Nucl Med. 1998;39(10):1690-6.

27. Takala TO et al. 14(R,S)-[18F]Fluoro-6-thia-heptadecanoic acid as a tracer of free fatty acid uptake and oxidation in myocardium and skeletal muscle. Eur J Nucl Med Mol Imaging. 2002;29(12): 1617-22.

28. Ebert A et al. Kinetics of 14(R,S)-fluorine-18-fluoro-6-thia-heptadecanoic acid in normal human hearts at rest, during exercise and after dipyridamole injection. J Nucl Med. 1994;35(1):51-6.

29. Schulz G et al. Imaging of beta-oxidation by static PET with 14(R,S)-[18F]-fluoro-6-thiaheptadecanoic acid (FTHA) in patients with advanced coronary heart disease: A comparison with 18FDG-PET and 99Tcm-MIBI SPET. Nucl Med Commun. 1996;17(12):1057-64.

30. Mäki MT et al. Free fatty acid uptake in the myocardium and skeletal muscle using fluorine-18-fluoro-6-thia-heptadecanoic acid. J Nucl Med. 1998;39(8):1320-7.

31. Ohira H et al. Shifts in myocardial fatty acid and glucose metabolism in pulmonary arterial hypertension: A potential mechanism for a maladaptive right ventricular response. Eur Heart J Cardiovasc Imaging. 2016;17(12):1424-31.

32. DeGrado TR et al. Synthesis and preliminary evaluation of (18)F-labeled 4-thia palmitate as a PET tracer of myocardial fatty acid oxidation. Nucl Med Biol. 2000;27(3):221-31.

33. DeGrado TR et al. Validation of 18F-fluoro-4-thia-palmitate as a PET probe for myocardial fatty acid oxidation: Effects of hypoxia and composition of exogenous fatty acids. J Nucl Med. 2006;47(1):173-81.

34. Mather KJ et al. Assessment of myocardial metabolic flexibility and work efficiency in human type 2 diabetes using 16-[18F]fluoro-4-thiapalmitate, a novel PET fatty acid tracer. Am J Physiol Endocrinol Metab. 2016;310(6):E452-60.

35. Shoup TM et al. Evaluation of trans-9-18F-fluoro-3,4-methyleneheptadecanoic acid as a PET tracer for myocardial fatty acid imaging. J Nucl Med. 2005;46(2): 297-304.

36. Gheysens O et al. Quantification of myocardial perfusion in humans by PET/CT and the fatty acid analogue 18F-FCPHA: A feasibility study. J Nucl

Med. 2014;55(Suppl1):1770.

37. Levy MN, Zieske H. Autonomic control of cardiac pacemaker activity and atrioventricular transmission. J Appl Physiol. 1969;27(4):465-70.

38. Lymperopoulos A et al. Adrenergic nervous system in heart failure: Pathophysiology and therapy. Circ Res. 2013;113(6):739-53.

39. Triposkiadis F et al. The sympathetic nervous system in heart failure physiology, pathophysiology, and clinical implications. J Am Coll Cardiol. 2009;54(19):1747-62.

40. Parati G, Esler M. The human sympathetic nervous system: Its relevance in hypertension and heart failure. Eur Heart J. 2012;33(9):1058-66.

41. Travin MI. Current clinical applications and next steps for cardiac innervation imaging. Curr Cardiol Rep. 2017;19(1):1.

42. Pacholczyk T et al. Expression cloning of a cocaine- and antidepressant-sensitive human noradrenaline transporter. Nature. 1991;350(6316):350-4.

43. Jacobson AF et al. 123I-mIBG scintigraphy to predict risk for adverse cardiac outcomes in heart failure patients: Design of two prospective multicenter international trials. J Nucl Cardiol. 2009;16(1):113-21.

44. Narula J et al. 123I-MIBG imaging for prediction of mortality and potentially fatal events in heart failure: The ADMIRE-HFX study. J Nucl Med. 2015;56(7):1011-8.

45. Nakajima K, Nakata T. Cardiac 123I-MIBG imaging for clinical decision making: 22-year experience in Japan. J Nucl Med. 2015;56 Suppl 4:11s-19s.

46. Rosenspire KC et al. Synthesis and preliminary evaluation of carbon-11-meta-hydroxyephedrine: A false transmitter agent for heart neuronal imaging. J Nucl Med. 1990;31(8):1328-34.

47. Fuller RW et al. Formation of alpha-methylnorepinephrine as a metabolite of metaraminol in guinea pigs. Biochem Pharmacol. 1981;30(20):2831-6.

48. Fallavollita JA et al. Regional myocardial sympathetic denervation predicts the risk of sudden cardiac arrest in ischemic cardiomyopathy. J Am Coll Cardiol. 2014;63(2):141-9.

49. Pietila M et al. Reduced myocardial carbon-11 hydroxyephedrine retention is associated with poor prognosis in chronic heart failure. Eur J Nucl Med. 2001;28(3):373-6.

50. Yu M et al. Evaluation of LMI1195, a novel 18F-labeled cardiac neuronal PET imaging agent, in cells and animal models. Circ Cardiovasc Imaging. 2011;4(4):435-43.

51. Sinusas AJ et al. Biodistribution and radiation dosimetry of LMI1195: first-in-human study of a novel 18F-labeled tracer for imaging myocardial innervation. J Nucl Med. 2014;55(9):1445-51.

52. Hu B et al. A practical, automated synthesis of meta-[(18)F]fluorobenzylguanidine for clinical use. ACS Chem Neurosci. 2015;6(11):1870-9.

53. Zhang H et al. Imaging the norepinephrine transporter in neuroblastoma: a comparison of [18F]-MFBG and 123I-MIBG. Clin Cancer Res. 2014;20(8):2182-91.

54. Zhang H et al. Synthesis and evaluation of 18F-labeled benzylguanidine analogs for targeting the human norepinephrine transporter. Eur J Nucl Med Mol Imaging. 2014;41(2):322-32.

55. Böhm M et al. Reduction of beta-adrenoceptor density and evaluation of positive inotropic responses in isolated, diseased human myocardium. Eur Heart J. 1988;9(8):844-52.

56. Brodde OE et al. Receptor systems affecting force of contraction in the human heart and their alterations in chronic heart failure. J Heart Lung Transplant. 1992;11(4 Pt 2):S164-74.

57. de Jong RM et al. Myocardial beta-adrenoceptor downregulation in idiopathic dilated cardiomyopathy measured in vivo with PET using the new radioligand (S)-[11C]CGP12388. Eur J Nucl Med Mol Imaging. 2005;32(4):443-7.

58. Eckberg DL et al. Defective cardiac parasympathetic control in patients with heart disease. N Engl J Med. 1971;285(16):877-83.

59. Binkley PF et al. Parasympathetic withdrawal is an integral component of autonomic imbalance in congestive heart failure: Demonstration in human subjects and verification in a paced canine model of ventricular failure. J Am Coll Cardiol. 1991;18(2):464-72.

60. Syrota A et al. Muscarinic cholinergic receptor in the human heart evidenced under physiological conditions by positron emission tomography. Proc Natl Acad Sci U S A. 1985;82(2):584-8.

61. Le Guludec D et al. Increased myocardial muscarinic receptor density in idiopathic dilated cardiomyopathy: An in vivo PET study. Circulation. 1997;96(10):3416-22.

62. Mazzadi AN et al. Muscarinic receptor upregulation in patients with myocardial infarction: a new paradigm. Circ Cardiovasc Imaging. 2009;2(5):365-72.

63. Behling A et al. Cholinergic stimulation with pyridostigmine reduces ventricular arrhythmia and enhances heart rate variability in heart failure. Am Heart J. 2003;146(3):494-500.

64. Gjerløff T et al. In vivo imaging of human acetylcholinesterase density in peripheral organs using 11C-donepezil: Dosimetry, biodistribution, and kinetic analyses. J Nucl Med. 2014;55(11):1818-24.

65. Egleton RD et al. Angiogenic activity of nicotinic acetylcholine receptors: Implications in tobacco-related vascular diseases. Pharmacol Ther. 2009;21(2):205-23.

66. Santanam N et al. Nicotinic acetylcholine receptor signaling in atherogenesis. Atherosclerosis. 2012;225(2):264-73.

67. Bucerius J et al. Feasibility of 2-deoxy-2-[18F]fluoro-D-glucose- A85380-PET for imaging of human cardiac nicotinic acetylcholine receptors in vivo. Clin Res Cardiol. 2006;95(2):105-9.

68. Bers DM. Cardiac excitation-contraction coupling. Nature. 2002;415(6868):198-205.

69. Abriel H. Roles and regulation of the cardiac sodium channel Na v 1.5: Recent insights from experimental studies. Cardiovasc Res. 2007;76(3):381-9.

70. Bodi I et al. The L-type calcium channel in the heart: the beat goes on. J Clin Invest. 2005;115(12):3306-17.

71. Amin AS et al. Cardiac ion channels in health and disease. Heart Rhythm. 2010;7(1):117-26.

72. Moric E et al. The implications of genetic mutations in the sodium channel gene (SCN5A). Europace. 2003;5(4):325-34.

73. Haase H et al. Expression of calcium channel subunits in the normal and diseased human myocardium. J Mol Med. 1996;74(2):99-104.

74. Hooker JM et al. Imaging cardiac SCN5A using the novel F-18 radiotracer radiocaine. Sci Rep. 2017;7:42136.

75. Valette H et al. Myocardial kinetics of the 11C-labeled enantiomers of the Ca2+ channel inhibitor S11568: An in vivo study. J Nucl Med. 2001;42(6):932-7.

76. Kolbitsch C et al. Cardiac and Respiratory Motion Correction for Simultaneous Cardiac PET/MR. J Nucl Med. 2017;58(5):846-852.